FePt Nanoparticles with a Narrow Composition Distribution Synthesized via Pyrolysis of Iron(III) Ethoxide and Platinum(II) Acetylacetonate

Soichiro Saita[†,§] and Shinya Maenosono*[,‡]

Mitsubishi Chemical Group Science and Technology Research Center, Inc. (MCRC), Kamoshida-cho, Aoba-ku, Yokohama, Kanagawa 227-8502, Japan, and Department of Chemical System Engineering, School of Engineering, The University of Tokyo, Hongo 7-3-1, Bunkyo-ku, Tokyo 113-8656, Japan

Received March 14, 2005. Revised Manuscript Received May 12, 2005

Equiatomic colloidal FePt nanoparticles (NPs) of 4.5-nm mean diameter were chemically synthesized using iron(III) ethoxide and platinum(II) acetylacetonate as precursors. All of the starting materials used in the synthesis were stable in air and had relatively low toxicity. Reaction proceeded without any reducing agent, providing an easy and robust way of synthesis of FePt NPs. FePt NPs were characterized by X-ray diffractometry (XRD), transmission electron microscopy (TEM), energy-dispersive X-ray fluorescence spectrometry (EDX), and inductively coupled plasma atomic emission spectrometry (ICP-AES). TEM-EDX analysis revealed that FePt NPs contained little oxygen or other impurities. In addition, the atomic composition distribution of each NP was considerably narrow, and seven out of ten NPs contained Fe and Pt atoms necessary to be transformed into the chemically ordered $L1_0$ crystalline structure. By annealing at 600 °C for 30 min, as-synthesized fcc FePt NPs were transformed into the $L1_0$ phase and showed coercivity of 11.2 kOe.

Introduction

Among many kinds of magnetic materials, $L1_0$-phase FePt shows almost the highest magnetic anisotropy, resulting in high coercivity.[1] Thus, FePt has been intensively studied as a material for magnetic recording media with a storage capacity of Tbit/in^2.[2] After the IBM group reported the synthesis of FePt nanoparticles (NPs) in liquid phase using iron pentacarbonyl [$Fe(CO)_5$] and platinum(II) acetylacetonate [$Pt(acac)_2$] as precursors,[3] a lot of groups investigated advanced synthetic methods[4−6] and applications of FePt NPs.[7−9] FePt shows a high maximum energy product $(BH)_{max}$ of 13 MGOe.[10] Therefore, FePt NPs are also attractive materials for medical or nanocomposite applications.[11,12] Additionally, FePt is a promising material as a catalyst for fuel cells.[13]

For the above-mentioned applications, there are several requirements for FePt NPs. First of all, although a smaller size is better, the diameter of NPs should be larger than the superparamagnetic limit, ∼3.3 nm, if one wants FePt NPs to be ferromagnetic.[14] Second, the size distribution of NPs should be narrow enough for the application. Third, undesirable sintering between each NP, that takes place when NPs are annealed in order to transform the crystalline structure from the chemically disordered fcc to the chemically ordered fct ($L1_0$ phase), should be avoided. Finally, the Fe_xPt_{100-x} NPs should be within the composition of $40 \leq x \leq 60$ to be transformed into the $L1_0$ structure according to the phase diagram.[15] Although various synthetic methods have been proposed to fulfill some of these requirements, to the best of our knowledge, to date, none of them succeeded in meeting all the requirements simultaneously. For example, in the case of the most popular synthetic method in which $Fe(CO)_5$ is used as a precursor,[3] besides the drawbacks of high toxicity and high flammability, the atomic composition distribution of FePt NPs (mean diameter 3 nm) is extremely broad and the fraction of Fe_xPt_{100-x} NPs which are within a composition of $40 \leq x \leq 60$ was reported to be less than 30%.[16] When iron(III) acetylacetonate[17] or iron(II) chloride[18] is chosen as a precursor, the reducing agent, such as a sodium

* Corresponding author. E-mail: shinya@chemsys.t.u-tokyo.ac.jp.
† Mitsubishi Chemical Group Science and Technology Research Center, Inc. (MCRC).
‡ The University of Tokyo.
§ E-mail: 1707607@cc.m-kagaku.co.jp.

(1) Weller, D.; Moser, A. *IEEE Trans. Magn.* **1999**, *35*, 4423.
(2) Sun, S.; Fullerton, E. E.; Weller, D.; Murray, C. B. *IEEE Trans. Magn.* **2001**, *37*, 1239.
(3) Sun, S.; Murray, C. B.; Weller, D.; Folks, L.; Moser, A. *Science* **2000**, *287*, 1989.
(4) Harpeness, R.; Gedanken, A. *J. Mater. Chem.* **2005**, *15*, 698.
(5) Zeng, Q.; Zhang, Y.; Wang, H. L.; Papaefthymiou, V.; Hadjipanayis, G. C. *J. Magn. Magn. Mater.* **2004**, *272*−*276*, e1223.
(6) Kang, S.; Jia, Z.; Shi, S.; Nikles, D. E.; Harrell, J. W. *Appl. Phys. Lett.* **2005**, *86*, 62503.
(7) Gu, H.; Ho, P. L.; Tsang, K. W. T.; Wang, L.; Xu, B. *J. Am. Chem. Soc.* **2003**, *125*, 15702.
(8) Willard, M. A.; Kurihara, L. K.; Carpenter, E. E.; Calvin, S.; Harris, V. G. *Int. Mater. Rev.* **2004**, *49*, 125.
(9) Yu, A. C. C.; Mizuno, M.; Sasaki, Y.; Inoue, M.; Kondo, H.; Ohta, I.; Djayaprawira, D.; Takahashi, M. *Appl. Phys. Lett.* **2003**, *82*, 4352.
(10) Zeng, H.; Li, J.; Liu, J. P.; Wang, Z. L.; Sun, S. *Nature* **2002**, *420*, 395.
(11) Gu, H.; Ho, P. L.; Tsang, K. W. T.; Yu, C. W.; Xu, B. *Chem. Commun.* **2003**, 1966.
(12) Rong, C. B.; Zhang, H. W.; Du, X. B.; Zhang, J. *J. Appl. Phys.* **2004**, *96*, 3921.
(13) Toda, T.; Igarashi, H.; Uchida, H.; Watanabe, M. *J. Electrochem. Soc.* **1999**, *146*, 3750.
(14) Weller, D.; Moser, A.; Folks, L.; Best, M. E.; Lee, W.; Toney, M. F.; Schwickert, M.; Thiele, J. U.; Doerner, M. F. *IEEE Trans. Magn.* **2000**, *36*, 10.
(15) Stahl, B.; Ellrich, J.; Theissmann, R.; Ghafari, M.; Bhattacharya, S.; Hahn, H.; Gajbhiye, N. S.; Kramer, D.; Viswanath, R. N.; Weissmuller, J.; Gleiter, H. *Phys. Rev. B* **2003**, *67*, 14422.
(16) Yu, A. C. C.; Mizuno, M.; Sasaki, Y.; Kondo, H. *Appl. Phys. Lett.* **2004**, *85*, 6242.

10.1021/cm050568c CCC: $30.25
Published on Web 06/09/2005

or boron compound, has to be used in the synthesis. A purification process is needed to remove such elements, otherwise these elements are included in the FePt NPs as impurities.[18] In addition, in many cases, only NPs smaller than the superparamagnetic limit (~3.3 nm) have been produced.[18−21] Although one can synthesize $L1_0$ FePt NPs directly using a polyol reduction method at high temperatures, the resulting NPs often tend to aggregate[22] and the quality of FePt NPs was inferior to that of those obtained by using $Fe(CO)_5$. Chen et al. succeeded in making 6-nm and 9-nm FePt NPs with a good average composition by controlling the heating rate and Ar gas flow rate precisely.[23] Moreover, they mentioned a little bit about the reaction mechanism.[23] However, the atomic composition distribution of NPs and the detailed reaction mechanism have not been clarified yet. Additionally, the synthesis procedure was complicated and the reaction was rather sensitive.

We have previously studied the chemical ordering of FePt NPs by laser annealing in order to obtain individually isolated $L1_0$ FePt NPs without sintering.[24] As a result, by irradiating a dispersion of FePt NPs with a pulsed laser, phase transition of NPs from fcc to $L1_0$ successfully took place without significant sintering. However, because the size of FePt NPs was about 2 nm which is less than the superparamagnetic limit, they did not show ferromagnetism. In that study, we found that NPs transformed into $L1_0$ by pulsed-laser annealing were a part of all NPs produced (the precise fraction was not clear). This might be because we synthesized FePt NPs by a method in which $Fe(CO)_5$ was used as a precursor and the resulting NPs had a broad composition distribution. In short, the fraction of Fe_xPt_{100-x} NPs, which were within a composition of $40 \leq x \leq 60$ and were able to be transformed into $L1_0$, might be less than 30%. Considering the above-mentioned results, one should synthesize FePt NPs with an average size larger than 3.3 nm and with a narrow composition distribution to increase the fraction of NPs with an ability to be transformed into the $L1_0$ phase in order to obtain individually isolated ferromagnetic FePt NPs.

In general, Pt content in FePt NP tends to increase with increasing NP size. Thus, a unique synthetic approach has been proposed to obtain large FePt NPs with an equiatomic composition by several groups. For example, Teng and Yang reported that they succeeded in synthesizing large (average diameter 17 nm) $Fe_{50}Pt_{50}$ NPs by making Pt/Fe_2O_3 core/shell NPs followed by annealing in reductive atmosphere.[25] The synthesis of Pt/Fe_2O_3 core/shell NPs was sequential. First, the Pt core was synthesized using $Pt(acac)_2$, and then the Fe_2O_3 shell was coated on the Pt core by a second injection of $Fe(CO)_5$ into the reaction system. In addition, this synthetic method required precise temperature regulation. Thus, the synthesis process became rather complicated. To precisely control the size and composition distribution among FePt NPs in these synthetic methods, it was important to know the thermal decomposition and/or the reduction rates of iron and platinum precursors as well as the nucleation and growth rates of FePt NPs. In addition, the gas−liquid equilibrium of an iron precursor had to be known if one used a volatile material as a precursor such as $Fe(CO)_5$. Unfortunately, we do not know much about all this.

Here, we report the synthesis of FePt NPs using iron(III) ethoxide [$Fe(OEt)_3$] and platinum(II) acetylacetonate [$Pt(acac)_2$] as precursors without any reducing agent. $Fe(OEt)_3$ is a brown powder at room temperature (nonvolatile) and is a highly reactive late transition metal alkoxide. $Fe(OEt)_3$ has previously been used for making iron oxide by the sol−gel technique[26] and is a less toxic, hard-to-oxidize, and easy-to-handle material. In addition, decomposition products of $Fe(OEt)_3$ are less toxic. For these reasons, the use of $Fe(OEt)_3$ as a precursor is suitable for industrialization. Equiatomic FePt NPs of 4.5-nm average diameter with good composition distribution were obtained by this synthetic method.

Experimental Section

FePt Nanoparticle Synthesis. Iron(III) ethoxide [$Fe(OEt)_3$, purity: 95%] was purchased from AZmax. Platinum(II) acetylacetonate [$Pt(acac)_2$, purity: 97%] was purchased from Strem Chemicals. Octyl ether (purity: 99%), oleic acid (90%), and oleylamine (70%) were purchased from Aldrich. All reagents were used without further purification. An amount of 1 mmol of $Fe(OEt)_3$, 0.5 mmol of $Pt(acac)_2$, 17 mL of octyl ether, 1.6 mL of oleic acid, and 1.7 mL of oleylamine were placed in a three-necked flask at ambient air. The color of the resulting mixture was brown. The molar ratio of Fe to Pt in the mother reaction solution was adjusted to 2. Note that no reducing agent was used. The flask was then evacuated to remove oxygen and volatile components from the reaction solution. After evacuation, the flask was purged three times by high-purity Ar. Subsequently, the temperature was raised to 297 °C with a heating rate of 20 °C/ min under an Ar atmosphere. At around 150 °C, white smoke billowed from the solution and the reactant turned black gradually. After 30 min of reaction at 297 °C, the flask was cooled to 50 °C and ethanol bubbled by N_2 was added into the flask. By centrifuging this mixture, a black powder was separated from the matrix. Then the powder was redispersed in hexane. Precipitation and redispersion processes were repeated three times to remove impurities completely. By this synthetic procedure, 50-mg FePt NPs capped with oleic acid were obtained. The average composition of FePt NPs was determined by inductively coupled plasma atomic emission spectrometry (ICP-AES; Jobin Yvon JY38-S). For thermal annealing, as-synthesized FePt NPs were deposited on a quartz substrate by casting and drying the NP/hexane dispersion several times. A uniform film of the obtained FePt NPs was placed in an electric furnace and annealed at 600 °C for 30 min in an Ar/H_2 (3:2) reduced atmosphere.

(17) Iwaki, T.; Kakihara, Y.; Toda, T.; Abdullah, M.; Okuyama, K. *J. Appl. Phys.* **2003**, *94*, 6807.
(18) Sun, S.; Anders, S.; Thomson, T.; Baglin, J. E. E.; Toney, M. F.; Hamann, H. F.; Murray, C. B.; Terris, B. D. *J. Phys. Chem. B* **2003**, *107*, 5419.
(19) Elkins, K. E.; Vedantam, T. S.; Liu, J. P.; Zeng, H.; Sun, S.; Ding, Y.; Wang, Z. L. *Nano Lett.* **2003**, *3*, 1647.
(20) Nakaya, M.; Tsuchiya, Y.; Ito, K.; Oumi, Y.; Sano, T.; Teranishi, T. *Chem. Lett.* **2004**, *33*, 130.
(21) Liu, C.; Wu, X.; Klemmer, T.; Shukla, N.; Yang, X.; Weller, D.; Roy, A. G.; Tanase, M.; Laughlin, D. *J. Phys. Chem. B* **2004**, *108*, 6121.
(22) (a) Jeyadevan, B.; Hobo, A.; Urakawa, K.; Chinnasamy, C. N.; Shinoda, K.; Tohji, K. *J. Appl. Phys.* **2003**, *93*, 7574. (b) Jeyadevan, B.; Urakawa, K.; Hobo, A.; Chinnasamy, N.; Shinoda, K.; Tohji, K.; Djayaprawira, D. D.; Tsunoda, M.; Takahashi, M. *Jpn. J. Appl. Phys.* **2003**, *42*, L350.
(23) Chen, M.; Liu, J. P.; Sun, S. *J. Am. Chem. Soc.* **2004**, *126*, 8394.
(24) Saita, S.; Maenosono, S. *J. Phys. Condens. Mater.* **2004**, *16*, 6385.
(25) Teng, X.; Yang, H. *J. Am. Chem. Soc.* **2003**, *125*, 14559.
(26) Armelao, L.; Granozzi, G.; Tondello, E.; Colombo, P.; Principi, G.; Lottici, P. P.; Antonioli, G. *J. Non-Cryst. Solids* **1995**, *192&193*, 435.

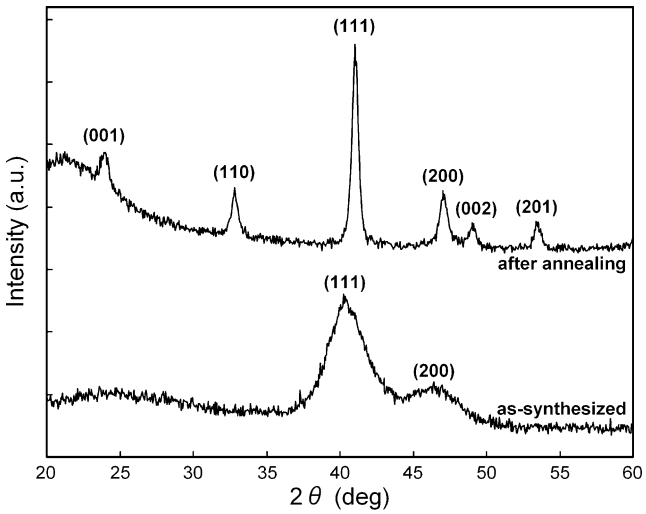

Figure 1. XRD patterns of FePt NPs before (bottom) and after (top) annealing.

XRD, TEM, TEM-EDX, and SAED. XRD patterns of FePt NPs were obtained in the reflection geometry using an X-ray diffractometer (Rigaku, RINT200PC) at room temperature with Cu Kα radiation (wavelength: 1.542 Å, incident angle: 1°, step width: 0.05°, counting time: 1 s). FePt NPs were deposited on glass substrates (Matsunami Micro Slide Glass, 8 × 10 mm^2) by casting and drying the NP/hexane dispersion for XRD measurements. High-resolution TEM micrographs of FePt NPs were obtained using a Hitachi H-9000UHR microscope operated at 300 kV. SAED patterns of FePt NPs were obtained using a FEI Tecnai G2 F20 microscope operated at 200 kV. TEM-EDX analysis was performed also using a FEI Tecnai G2 F20 microscope operated at 200 kV equipped with an EDAX Phoenix system. TEM-EDX analyses were carried out for single NPs and for a wide area containing 100−200 NPs.

Thermal Analysis. Thermo gravimetry-differential thermal analysis (TG-DTA; Seiko, TG/DTA320) was performed to investigate the thermal decomposition behavior of precursors using an electrical furnace (Seiko Instruments, SSC/5200). Quantities of 3.4 mg of $Fe(OEt)_3$, $Fe(acac)_3$, or $Pt(acac)_2$ were placed in a quartz cell, and the cell was placed in the furnace. The temperature was raised to 1000 °C with a heating rate of 20 °C/min under a N_2 atmosphere (flow rate 200 mL/min). Note that the heating rate was conformed to that of synthesis. Thermo gravimetry-mass spectrometry (TG-MS; Shimazu, TGMSdirect) was also carried out to determine the decomposition products of the precursors. A 3-mg sample of $Fe(OEt)_3$ was placed in a quartz cell, and the temperature was raised to 1000 °C with a heating rate of 20 °C/min under a He atmosphere (flow rate 100 mL/min). The decomposition products were then analyzed by mass spectrometry.

Magnetization Measurement. Magnetization curves of FePt NPs were obtained by using a vibrating sample magnetometer (VSM; RikenDenshi, BHV-50). In-plane measurements were performed at room temperature. Maximum applied field and frequency were 15 kOe and 28 Hz, respectively. FePt NPs were deposited on glass substrates by casting and drying the NP/hexane dispersion several times for magnetic measurements.

Results and Discussion

Figure 1 shows XRD patterns of FePt NPs before and after annealing. As shown in Figure 1, a crystalline structure of the as-synthesized NPs is a chemically disordered fcc phase.[3] The mean crystallite size was estimated to be 2.9 nm from the half-maximum full width of the (111) peak by the Scherrer formula.[27] The XRD pattern of FePt NPs after annealing was representative of a typical chemically ordered $L1_0$ phase. Lattice parameters (c and a parameters) were calculated to be $c = 3.711$ and $a = 3.855$ Å from the peak positions of (001) and (110) super lattice peaks, respectively. The c/a ratio which represents the tetragonality of FePt crystallite was $c/a = 0.963$. By de-convoluting the fundamental (200)/(002) peaks, c and a parameters were calculated to be $c = 3.713$ and $a = 3.857$ Å. In this case, the c/a was also $c/a = 0.963$. These values agreed well with the lattice constants of bulk $L1_0$ FePt ($c = 3.71$ and $a = 3.85$ Å).[28] Klemmer et al. systematically studied the lattice parameter changes of $L1_0$ FePt NPs annealed to near equilibrium as a function of composition by X-ray diffraction.[29] They found that the (111) peak position shows linear behavior with the Fe/Pt ratio of the precursor and it shifts to higher angles with increasing Fe content in FePt NP.[29] In addition, they also clarified the correlation between the c/a ratio and the magnetocrystalline anisotoropy.[29] As a result, one can estimate the Fe/Pt ratio, coercivity, and lattice parameters on the basis of the (111) peak position of $L1_0$ FePt NPs. The (111) peak position of annealed FePt NPs shown in Figure 1 is 41.04 degrees, which approximately corresponds to Fe/Pt = 55/45, $c = 3.73$, and $a = 3.86$ Å according to Klemmer et al.[29] Thus, the Fe/Pt atomic ratio of NPs is supposed to be equiatomic.

Figure 2, parts a and b, shows low- and high-magnification TEM micrographs of as-synthesized FePt NPs. Note that aggregation of NPs and extraneous substances are not seen in the field of view. Figure 2c is the SAED pattern of as-synthesized FePt NPs taken from a region of 800-nm diameter. The (111) and (200) rings of the fcc-phase FePt crystallite are clearly seen. TEM and SAED observations revealed that crystallite growth was good, but crystallinity was not very good because a number of lattice defects were observed as shown in the inset of Figure 2b. Figure 2d shows the size distribution of as-synthesized FePt NPs that was estimated from randomly selected 300 NPs from the TEM image (Figure 2a). The mean diameter was estimated to be 4.5 nm, which is larger than the lowest limit for showing coercivity for more than 10 years (∼3.3 nm).[14] Standard deviation of the size distribution was 16%, which was relatively broad compared with that of FePt NPs synthesized via other existing routes (5−10%).[3,18−21] By tuning reaction conditions or by using a size-separation technique, the size distribution would become narrow and similar to that of NPs synthesized via preexisting methods. For example, in the case of FeMo NP synthesis, mean size and size distribution of NPs were significantly varied by changing the molar ratio of octanoic acid to bis-2-ethylhexylamine, which were added as protective agents.[30] This technique could also be appropriate in our system to minimize the size distribution of NPs.

(27) Nair, P. S.; Radhakrishnan, T. R.; Revaprasadu, N.; Kolawole, G.; O'Brien, P. *J. Mater. Chem.* **2002**, *12*, 2722.
(28) Powder Diffraction File 43-1359; International Center for Diffraction Data, Newtown Square, PA, 1994.
(29) Klemmer, T. J.; Shukla, N.; Liu, C.; Wu, X. W.; Svedberg, E. B.; Mryasov, O.; Chantrell, R. W.; Weller, D.; Tanase, M.; Laughlin, D. E. *Appl. Phys. Lett.* **2002**, *81*, 2220.
(30) Li, Y.; Liu, J.; Wang, Y.; Wang, Z. L. *Chem. Mater.* **2001**, *13*, 1008.

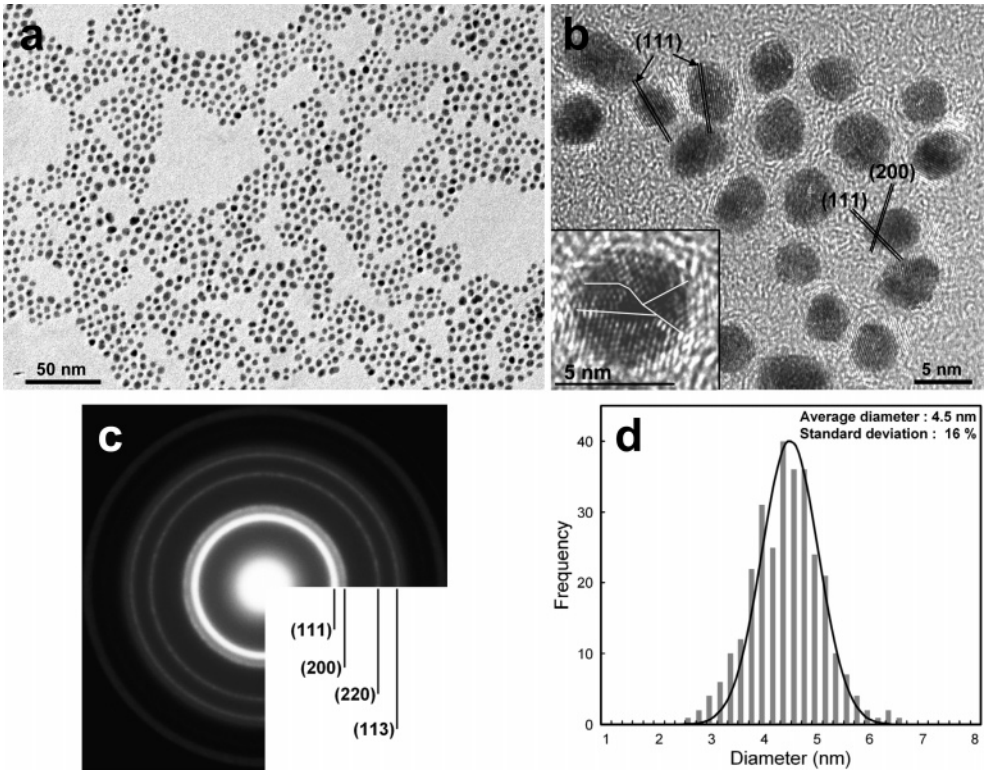

Figure 2. (a) Low- and (b) high-magnification TEM micrographs of as-synthesized FePt NPs. The inset shows the high-resolution TEM micrograph of the defects on a single FePt NP. (c) SAED pattern and (d) size distribution of as-synthesized fcc-FePt NPs. The solid line represents the Gaussian distribution which fitted the histogram.

Atomic composition of each single NP was analyzed by TEM-EDX to evaluate the composition distribution. A quantity of 23 randomly selected NPs were examined by TEM-EDX. At the same time, an average composition of 100−200 NPs was also examined by wide-field EDX analysis. Figure 3, parts a and b, shows EDX spectra of NPs having the lowest ($Fe_{30.5}Pt_{69.5}$) and the highest ($Fe_{61.2}Pt_{38.8}$) Fe content among the 23 NPs, respectively. Figure 3c represents the wide-field EDX spectrum. The average composition of 100−200 NPs was $Fe_{56.6}Pt_{43.4}$. This value agreed well with the composition estimated from lattice parameters as mentioned above. Note that Cu peaks seen in Figure 3 are from the TEM grid. Intensity of the oxygen peak in Figure 3 is similar to the background level (data not shown). Hence, we conclude that iron oxide does not exist in NPs. ICP-AES analysis also confirmed that the average composition of the NP ensemble was $Fe_{50}Pt_{50}$, which agrees with the TEM-EDX elemental analytical results. Thus, we conclude that the FePt NPs synthesized have an equiatomic composition in average.

Fe_xPt_{100-x} NPs should be within the composition of $40 \leq x \leq 60$ to be transformed into the $L1_0$ phase from a thermodynamical point of view as mentioned above. Figure 4 shows the composition distribution obtained from 23 NPs individually analyzed by TEM-EDX. From the histogram, the fraction of Fe_xPt_{100-x} NPs, which were within a composition of $40 \leq x \leq 60$ (ϕ_{40-60}) was calculated to be 74%. On the other hand, ϕ_{40-60} was 82% from the Gaussian distribution function which fitted the histogram. This value was more than 2.5 times higher than the value reported previously.[16] However, the 23 NPs were too scarce to precisely determine the composition distribution of the parent population (over

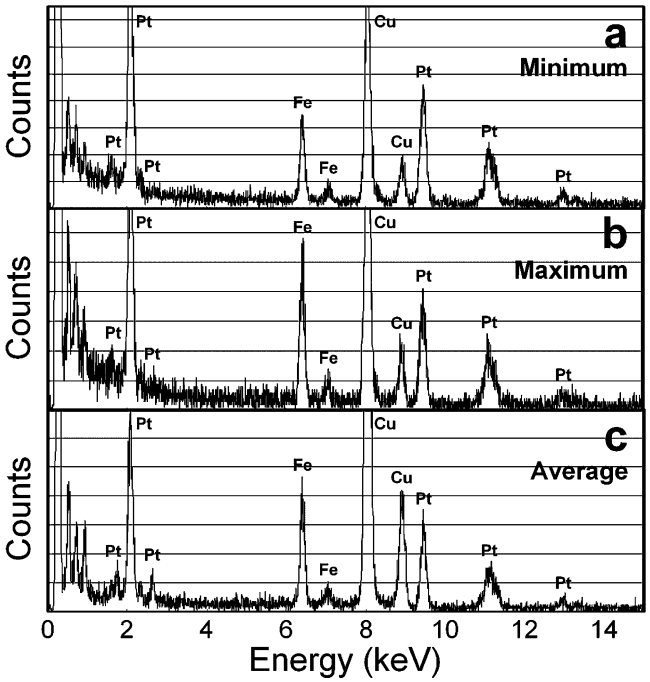

Figure 3. EDX spectra of single NPs having (a) the lowest ($Fe_{30.5}Pt_{69.5}$) and (b) the highest ($Fe_{61.2}Pt_{38.8}$) Fe content among the 23 NPs. (c) Wide-field EDX spectrum from 100 to 200 NPs. The average composition of 100−200 NPs is $Fe_{56.6}Pt_{43.4}$.

500 NPs should be analyzed to estimate the distribution of a parent population).[16] Nevertheless, ϕ_{40-60} was considerably larger than 30% in our case, because it is extremely rare to find seven out of ten NPs having a composition of $40 \leq x \leq 60$ from randomly selected 23 NPs if $\phi_{40-60} \leq 30\%$. Let us suppose that the composition distribution of the parent population of FePt NPs obeyed the Gaussian distribution.

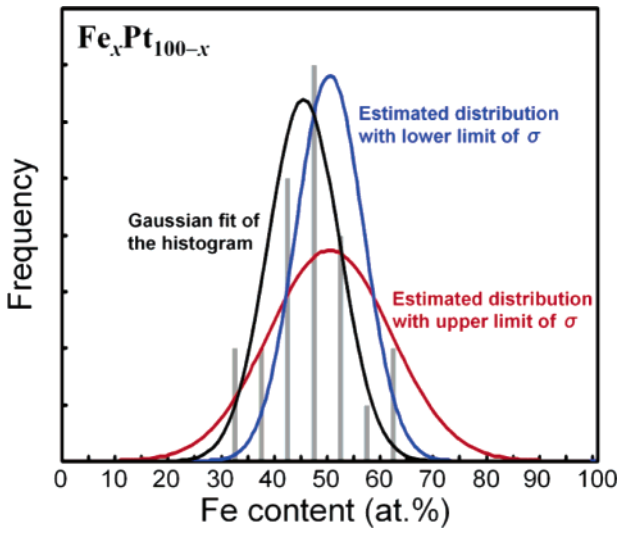

Figure 4. Composition distribution obtained from 23 NPs individually analyzed by TEM-EDX. Black curve is the Gaussian fit of the histogram. Red and blue curves, respectively, represent the estimated broadest and narrowest distributions of the parent population with 95% confidence level. Note that these two curves are normalized in order that the area equates to that of the Gaussian fit of the histogram (black curve).

In that case, the relationship between the population variance σ^2 and the sample variance S^2 would be

$$\sigma^2 = \frac{(n-1)S^2}{\chi^2} \tag{1}$$

where n and χ^2 are the number of samples and the chi-square distribution, respectively. The 95% confidence interval of σ^2 can be written as

$$\frac{(n-1)S^2}{{\chi_{0.025}}^2} \le \sigma^2 \le \frac{(n-1)S^2}{{\chi_{0.975}}^2} \tag{2}$$

where ${\chi_{0.025}}^2$ and ${\chi_{0.975}}^2$ represent 2.5% points of right and left side of χ^2 distribution, respectively. According to eq 2, we estimated the upper and lower limits of the population variance (σ_{max} and σ_{min}). In consequence, we obtained $\sigma_{max} = 11.5$ and $\sigma_{min} = 6.3$ ($S^2 = 65.48$, ${\chi_{0.025}}^2 = 36.78$, and ${\chi_{0.975}}^2 = 10.98$). By using σ_{max} and σ_{min}, and assuming that the mean composition was $Fe_{50}Pt_{50}$, we calculated the composition distribution of the parent population. In Figure 4, the broadest (red curve) and the narrowest (blue curve) distributions are shown. In the broadest and narrowest distributions, $\phi_{40-60} = 69\%$ and $\phi_{40-60} = 97\%$, respectively. These results indicate, with 95% confidence level, that ϕ_{40-60} is larger than 69% even in the parent population. Hence, there is no doubt that the composition distribution was markedly improved compared with that of FePt NPs synthesized via an $Fe(CO)_5$ precursor.

Although iron is easily oxidized, TEM-EDX analysis revealed that almost no iron oxide was included in NPs despite the fact that $Fe(OEt)_3$ has three Fe−O bonds in one molecule. Thus, we investigated how $Fe(OEt)_3$ decomposed and participated in the reaction by using TG-DTA and TG-MS analyses. Just after the beginning of heating (~50 °C), a weight loss started to be observed and it remained constant up to around 300 °C, which was just above the maximum

Scheme 1. Reaction Model for FePt Nanoparticle Formation via $Fe(OEt)_3$ Decomposition and $Pt(acac)_2$ Reduction

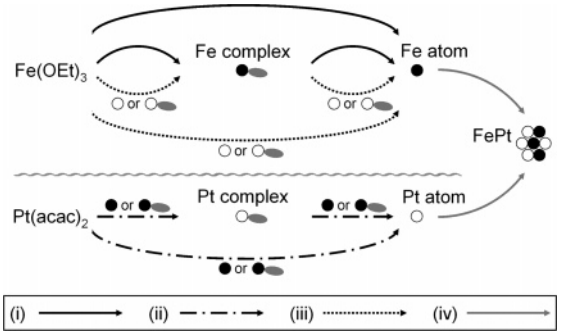

temperature in the reaction. TG-MS analysis revealed that the main decomposition product of $Fe(OEt)_3$ was ethanol (>90%). No evaporation or sublimation of $Fe(OEt)_3$ was detected. Neither ethane nor ethylene was detected. On the basis of these results, we hypothesized that ethoxide ligands detached from $Fe(OEt)_3$. The β-hydride elimination is a well-known reaction for thermal decomposition of late transition metal alkoxides.[31,32] In the case of $Fe(OEt)_3$, a β-hydrogen in one ethoxide ligand would be transferred to the Fe atom followed by a coordination of H-lacking ethoxide residue (acetaldehyde) on the Fe atom and an elimination of one ethanol molecule.[31] In the actual reaction system, there was a large amount of oleic acid which is a coordinative molecule. Thus, the remaining acetaldehyde ligands may be exchanged with oleic acid and immediately discharged to the outside of the reaction system. For comparison, $Fe(acac)_3$ and $Pt(acac)_2$ were also analyzed by TG-DTA. Unlike $Fe(OEt)_3$, $Fe(acac)_3$ showed no decomposition up to around 190 °C. $Pt(acac)_2$ also showed no decomposition up to 210 °C.

Considering these results, we propose the reaction model shown in Scheme 1. After heating has started, (i) a part of ethoxide ligands detaches from $Fe(OEt)_3$ by β-hydride elimination, and Fe complexes (or Fe atoms) and ethanol are generated. Subsequently, (ii) Fe complexes (or Fe atoms) formed by the decomposition of $Fe(OEt)_3$ catalyze the reduction of $Pt(acac)_2$, and Pt atoms are formed. Fe and Pt belong to the same family in the periodic table and have similar chemisorption energy.[33] Fe is slightly more reactive than Pt and, for example, is used as a reduction catalyst in traditional Fischer−Tropsch synthesis.[34] For these reasons, it is not wrong to propose that Fe (or Fe complexes) catalyzes the reduction of $Pt(acac)_2$ in our system. Then, (iii) Pt complex acts as a catalyst for the decomposition of $Fe(OEt)_3$ (or Fe complexes) and reaction i proceeds. It is reported that Pt cations can play a critical role in inducing and accelerating the reduction of associated metal cations.[22] Thus, Fe salt can be reduced to the neutral state when both Fe salt and Pt salt simultaneously exist in the system.[35] Finally, (iv) nucleation takes place in which Fe and Pt atoms are simultaneously

(31) Bryndza, H. E.; Calabrese, J. C.; Marsi, M.; Roe, D. C.; Tam, W.; Bercaw, J. E. *J. Am. Chem. Soc.* **1986**, *108*, 4805.
(32) Dongare, M. K.; Sinha, A. P. B. *Thermochim. Acta* **1982**, *57*, 37.
(33) Anderson, A. B. *Surf. Sci.* **1981**, *105*, 159.
(34) Bai, L.; Xiang, H. W.; Li, Y. W.; Han, Y. Z.; Zhong, B. *Fuel* **2002**, *81*, 1577.
(35) Liu, C.; Wu, X.; Klemmer, T.; Shukla, N.; Weller, D.; Roy, A. G.; Tanase, M.; Laughlin, D. *Chem. Mater.* **2005**, *17*, 620.

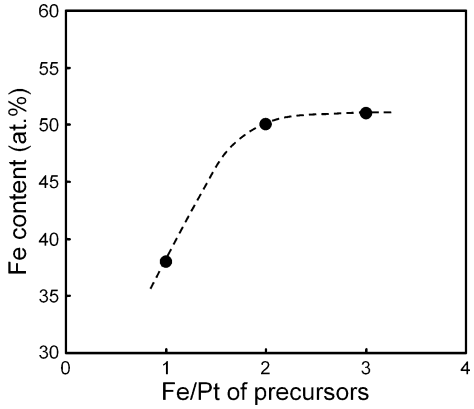

Figure 5. Average composition of Fe_xPt_{100-x} NPs plotted versus the molar ratio of Fe to Pt in the mother reaction solution. The dashed line is drawn as a guide.

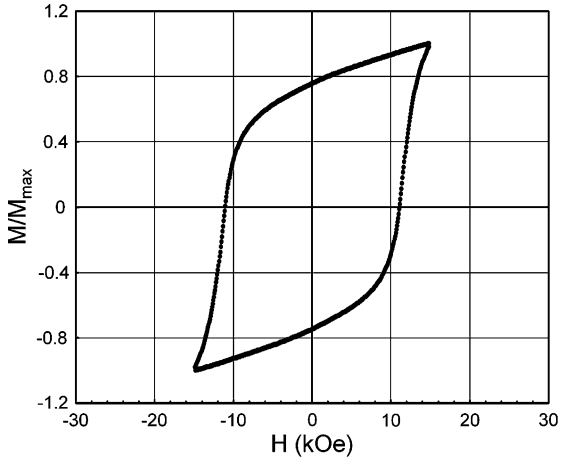

Figure 6. Magnetization curve of $L1_0$-phase FePt NPs after annealing.

incorporated, and then FePt NPs form. Here, reaction iii is not always necessary. However, if reaction iii exists in the reaction scheme, the reaction proceeds autocatalytically. In the case of the synthetic method in which $Fe(CO)_5$ is used as a precursor, thermal decomposition of $Fe(CO)_5$ and reduction of $Pt(acac)_2$ would proceed simultaneously. Importantly, a major portion of $Fe(CO)_5$ exists in the vapor phase because the boiling point of $Fe(CO)_5$ is much lower than the decomposition temperature. Thus, $Fe(CO)_5$ in the vapor phase is continuously supplied to the liquid phase by reflux during the reaction. However, the amount of reflux is generally uncontrollable. This leads to a significant spatio-temporal inhomogeneity of $Fe(CO)_5$ concentration in the reaction system. On the other hand, reduction of $Pt(acac)_2$ by diol molecules proceeds independently and would be accelerated in a certain temperature range. An imbalance between $Fe(CO)_5$ decomposition and $Pt(acac)_2$ reduction may cause a broad composition distribution of NPs. In our case, it is possible to explain the narrow composition distribution on the basis of the reaction model shown in Scheme 1. Thermal decomposition of $Fe(OEt)_3$ acts as a trigger for the reduction of $Pt(acac)_2$. In other words, $Fe(OEt)_3$ decomposition and $Pt(acac)_2$ reduction reactions are linked. In addition, evaporation of $Fe(OEt)_3$ is negligible, and thus the stable reaction continues, followed by nucleation of FePt NPs. According to this scenario, the synthetic route using $Fe(OEt)_3$ and $Pt(acac)_2$ as precursors without any reducing agent is robust enough in view of a composition control.

Figure 5 shows the average composition of Fe_xPt_{100-x} NPs obtained by ICP-AES plotted versus the molar ratio of Fe to Pt in the mother reaction solution. The input molar ratio of Fe to Pt was changed to 1, 2 (standard condition), and 3 by keeping the concentration of $Pt(acac)_2$ in the reaction solution constant. The average Fe content increased with an increase in the input molar ratio of Fe to Pt. When the input Fe/Pt ratios were 1, 2, and 3, average compositions were $Fe_{38}Pt_{62}$, $Fe_{50}Pt_{50}$, and $Fe_{51}Pt_{49}$, respectively. These results indicated that the composition of FePt NPs was easily tuned by the input Fe/Pt ratios. However, as shown in Figure 5, the Fe content in the NPs was saturated when the input Fe/Pt ratio was larger than 2. The reason for this behavior is unclear, and further investigation is needed to understand the reaction mechanism in this system.

Finally, the magnetization curve of FePt NPs after annealing is shown in Figure 6. The annealed $L1_0$-phase FePt NPs exhibited a coercivity of 11.2 kOe at room temperature. FePt NPs before annealing were superparamagnetic, which is typically representative of fcc-phase FePt NPs (data not shown). As seen in Figure 6, the magnetization curve does not saturate because the maximum applied field of VSM used in this study was 15 kOe. Thus, the actual coercivity would be larger than 11.2 kOe. According to Klemmer et al.,[29] coercivity of about 12 kOe (at room temperature) is expected when the (111) peak position of the $L1_0$-phase FePt NPs in an XRD pattern is 41.04 degrees, which approximately corresponds to Fe/Pt = 55/45, $c = 3.73$, and $a = 3.86$ Å as mentioned above. Thus, our results are consistent with those of Klemmer et al.[29]

Conclusion

By using iron(III) ethoxide [$Fe(OEt)_3$] and platinum diacetylacetonate [$Pt(acac)_2$] as precursors, monodispersed equiatomic colloidal FePt nanoparticles (NPs) of 4.5-nm mean diameter were chemically synthesized without a reducing agent. TEM-EDX analysis of single NPs revealed that the composition distribution among NPs was much narrower than that of NPs synthesized via a conventional method using iron pentacarbonyl as an Fe precursor. The fraction of Fe_xPt_{100-x} NPs, which were within an appropriate composition range to be transformed into the $L1_0$ phase, was found to be over 70%. The reason such narrowed composition distribution was obtained might be related to synchronization between thermal decomposition of $Fe(OEt)_3$ and reduction of $Pt(acac)_2$. By annealing FePt NPs at 600 °C for 30 min, as-synthesized fcc-phase FePt NPs were transformed into the $L1_0$-phase and showed coercivity of 11.2 kOe. The synthetic route proposed in this study is easy and robust enough in view of a composition control compared with other existing methods. Moreover, the precursor is less toxic and easy-to-handle. The mean-size control and the further size distribution narrowing remained as unresolved issues.

Acknowledgment. We thank Dr. Takashima (MCRC) for the high-resolution TEM observations. We also thank Dr. Asatani (MCRC) for carefully reading the manuscript.

CM050568C